Modular Linear Ion Source

H.R. Kaufman, J.R. Kahn, and R.E. Nethery
Kaufman & Robinson, Inc., Fort Collins, Colorado 80524

Key Words: Ion source; Ion beam assisted deposition; Ion beam sputtering; Ion beam cleaning

ABSTRACT

The modular linear ion source described herein uses cylindrical end-Hall modules in a linear array. The modules are operated in parallel so that there is a single gas flow to the ion source, a single discharge power supply, and a single hollow-cathode electron source, similar to a non-modular design. The spacing between the modules can be varied to obtain a wide range of operating characteristics while keeping a high degree of ion-dose uniformity along the length. The ion beam is fully neutralized to provide stable operation that is not dependent on workpiece material.

INTRODUCTION

Gridless sources are widely used for cleaning, etching, and ion-beam-assisted deposition. Cylindrical configurations of these sources [1-3] have been cost-effective and reliable in production applications, but these advantages have been more difficult to realize for linear ion-source configurations (see Fig. 1). Problems associated with conventional linear ion sources have included high gas consumption, lack of flexibility in ion-beam lengths, and warping and relative motion of adjoining parts due to substantial accumulated thermal expansion.

The modular linear ion source described herein (see Fig. 2) uses cylindrical modules of the end-Hall type. It is economical in its consumption of gas and is easily adjusted to fit a wide range of beam lengths and ion-dose requirements. At the same time, only one discharge supply, one ion-source gas-flow control, and one cathode-neutralizer are required (see Fig. 3).

GAS FLOW

The gas flow required for an ion source has two major components, the flow required to generate the ions and the flow required to sustain the discharge. Most ions generated by ion sources are singly ionized. The gas flow required to generate the ions can therefore be estimated from the number of gas molecules per standard cubic centimeter and the singly ionized nature of the molecules. (If the gas is oxygen or nitrogen, for example, the ions are mostly O_2^+ or N_2^+.) The ion charge per standard cubic centimeter of gas equals the product of the number of molecules per standard cubic centimeter (2.69×10^{19}) and the electronic charge (1.60×10^{-19} C), or 4.30 C/cm^3. About 14 sccm is therefore required to generate one ampere of ion-beam current.

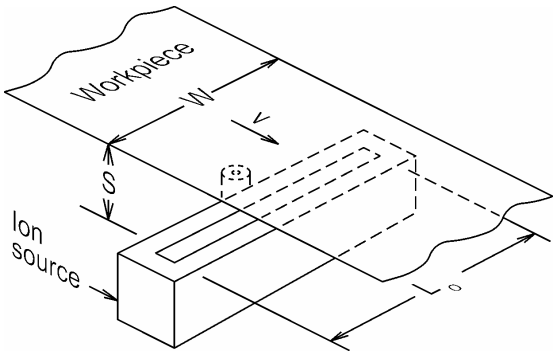

Figure 1. Installation of linear end-Hall ion source.

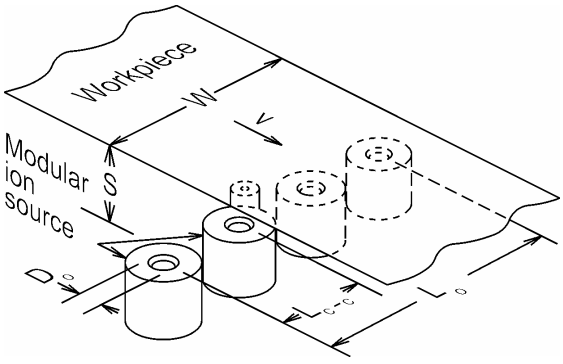

Figure 2. Installation of modular linear end-Hall ion source.

The gas flow to sustain the discharge requires more explanation. A qualitative understanding of this gas flow can be had by considering the lifetime and replacement of a single ion in the quasineutral discharge plasma. For a

47th Annual Technical Conference Proceedings (2004) ISSN 0737-5921

steady-state discharge, the background pressure of neutral gas molecules must be high enough for the electron that charge neutralizes that single ion to generate a new ion, during the time that the ion is moving from an average location in the discharge where it was generated to a boundary of the discharge region. If this distance is increased, there is more time for the electron to generate a new ion and the gas pressure can be lower. The minimum neutral gas loss is proportional to the product of this minimum pressure and the area through which the neutral gas can escape. Keep in mind that this is the *minimum* loss rate of neutrals. It is usually possible to operate with a higher neutral loss rate by selecting specific operating parameters such as a low discharge voltage.

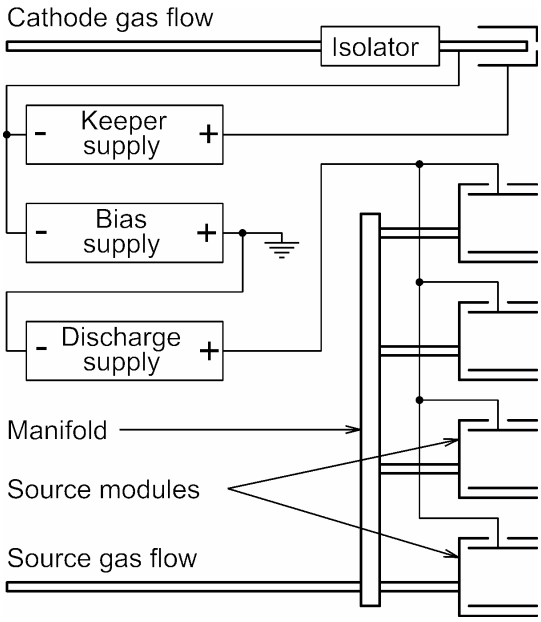

Figure 3. Schematic diagram of modular linear end-Hall ion source.

The neutral gas loss required to sustain the discharge has been studied for axisymmetric [4] and linear [5] discharge regions. Assuming a consistent design approach, the neutral gas loss from a single ion source is approximately proportional to the largest transverse dimension of the ion beam - the nominal ion beam length (L_o in Fig. 1) for a linear source and the nominal beam diameter (D_o in Fig. 2) for a circular source. If the sum of the diameters, D_o, for a modular linear source is much less than the beam length, L_o, for an equivalent linear source, the neutral gas loss from the modular linear source will be less than that from the linear ion source. The neutral gas loss from a linear end-Hall ion source depends on the operating conditions, but can easily be half of the total gas flow when operating on argon.

DESIGN CALCULATIONS

Uniform processing across the width W of the workpiece (see Fig. 1 and 2) is important. This workpiece moves past the ion source with a velocity, v. The side facing the ion source is processed by the ion beam. The process can be cleaning, etching, or ion-assisted deposition [6,7]. The integrated ion dose received by the workpiece, and the uniformity of this dose across the width, W, of the workpiece, are important process parameters. The integrated dose, typically in mA-s/cm^2, is

$$Dose = (1/v) \int i \, dy \qquad (1)$$

where v is the workpiece velocity in cm/s, i is the current density at the workpiece surface in mA/cm^2, and y is the distance measured parallel to the velocity, v. The integration is performed from a long distance before the ion source to a long distance after it. The velocity v is application dependent, while the integral depends on the ion source. The integral is therefore the portion of Eq. (1) of interest here. The integral has the units of mA/cm, and must be evaluated for each location along the ion beam length, L_o. The variation of this integral along the ion beam is the measure of process uniformity, which, together with the mean value of ion current per unit length and the mean value of ion energy, characterizes a linear ion source.

The distribution of ion current density from each module was assumed to follow

$$i = i_o \cos^n \Theta \qquad (2)$$

where i is ion current density at an angle Θ from the axis of the ion source, i_o is the ion current density at the same distance from the ion source but on the ion-source axis, and n is the beam-shape parameter [2,8]. The distribution of Eq. (2) is shown graphically in Fig. 4 for typical values of beam-shape parameter, n, from 1-4. The other elements of the ion source modeling include the inverse-square variation of ion current density with distance and the cosine correction for an oblique arrival at the workpiece surface. The ion current densities from the individual ion-source modules were summed to obtain the total ion current density for the integral at each location along the ion beam.

The variation of the integral of Eq. (1) along the ion beam length is shown as a departure from the mean value in Figs. 5-7. The number of ion-source modules was assumed to be eight, although the curves shown in Figs. 5-7 can be used to estimate the variations for a number of modules either

47th Annual Technical Conference Proceedings (2004) ISSN 0737-5921

greater or smaller than eight. Because the variations are symmetrical about the center of the ion beam, they are only shown for one half of the beam in these figures.

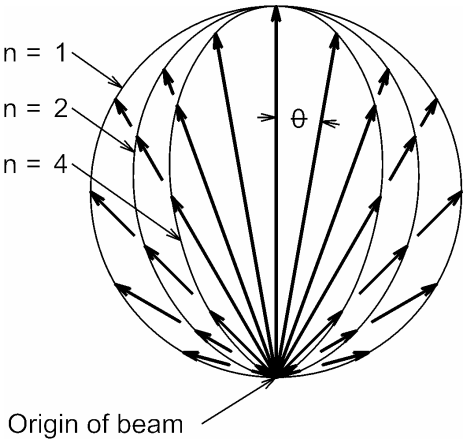

Figure 4. The distribution of ion current density for different values of beam-shape parameter. (The length of an arrow from the origin indicates the intensity in that direction.)

Figure 5 shows the effect of workpiece distance, S, relative to the center-to-center spacing between ion-source modules, $L_{c\text{-}c}$, for a beam-shape parameter, n, equal to 2. Increasing the value of $S/L_{c\text{-}c}$ decreases the variation in linear distribution in ion current between ion sources, but increases the fall-off near the end of the array, near module 1. The departure from the mean value is less than several percent over most of the beam length for values of $S/L_{c\text{-}c}$ of ≥1. Note that the units of distance from the center of the array are equal to the center-to-center spacing of the modules, and are not limited to any particular value.

Figure 6 shows the effect of beam-shape parameter, n, for a ratio of $S/L_{c\text{-}c}$ equal to 1.0. There is a general similarity of Figs. 5 and 6 in that an increase in n has an effect similar to a decrease in $S/L_{c\text{-}c}$. This means that, for sources and operating conditions that result in higher values of n, larger values of $S/L_{c\text{-}c}$ will be required for the same uniformity.

In Fig. 7 the beam-shape parameter, n, is equal to 2 and the ratio, $S/L_{c\text{-}c}$, is equal to 1.0. The spacing between modules 1 and 2 is changed from the same as the other modules (the bottom curve) to 90% of that value (the middle curve) to 80% of that value (the top curve). The uniformity for the center part of the array is about ±3% for all three curves. The bottom curve drops out of this band at about 1.9 units from the center. The top curve rises out of this band at about 2.3 units from the center.

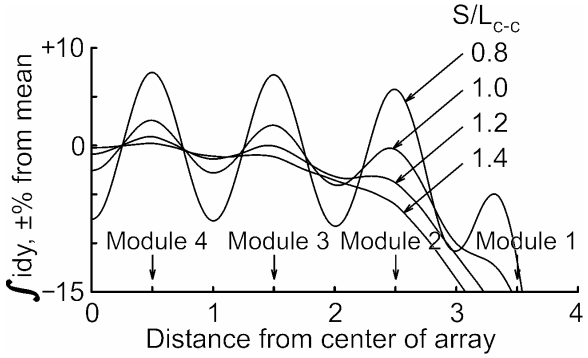

Figure 5. Effect of the ratio, $S/L_{c\text{-}c}$, on the dose uniformity for a modular linear end-Hall ion source. Beam-shape parameter, n, equals 2.

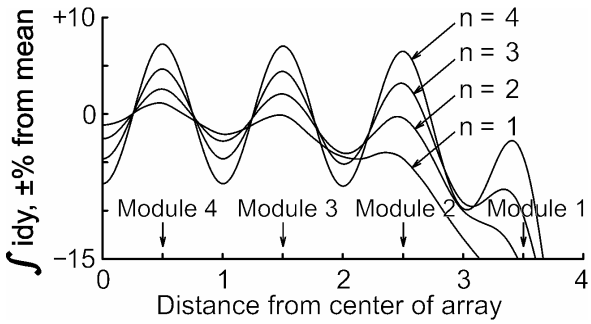

Figure 6. Effect of the beam-shape parameter, n, on the dose uniformity for a modular linear end-Hall ion source. The ratio, $S/L_{c\text{-}c}$, equals 1.0.

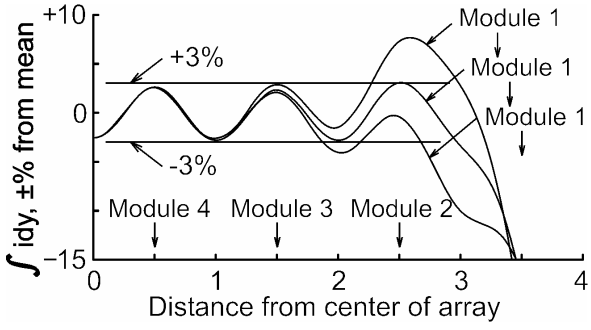

Figure 7. Effect of changing the center-to-center spacing of the end ion-source modules on the length of the uniform region. The beam-shape parameter, n, equals 2 and the ratio, $S/L_{c\text{-}c}$, equals 1.0.

47th Annual Technical Conference Proceedings (2004) ISSN 0737-5921

The middle curve in Fig. 7 shows near-optimum correction for the falloff near the end of the array by staying within the ±3% band until about 3.0 units from the center. A correction could also have been made by increasing the discharge current (hence the ion beam current) of the end modules above the value used for the other modules. However done, small corrections near the end of the array can extend the uniform region of processing.

An additional conclusion can be drawn from Fig. 7. Varying the spacing between modules 1 and 2 had a substantial effect at module 2, but little effect at module 3. Stated differently, for the combination of n and $S/L_{c\text{-}c}$ shown in Fig. 7, a change at one module has a significant effect at the next module, but very little effect at the next-nearest module. The curves to the right of module 3 are therefore close to what should be expected for half of the symmetrical variation from a five module array. Conversely, adding modules to the center of a five-or-greater module array, at the same center-to-center spacing, should simply continue to reproduce the variation shown between modules 3 and 4.

Depending on the specific value of beam-shape parameter, n, values of $S/L_{c\text{-}c}$ from about 1.0 to 1.5 should give processing that departs only several percent from a mean value and extends over a length within about one unit of center-to-center spacing, $L_{c\text{-}c}$, of the maximum center-to-center length of the array, L_o.

PERFORMANCE OF ION SOURCE MODULES

The ion-source module used has a diameter of 64 mm, a length of 51 mm, and was operated at a discharge power of 300 W [9]. The hollow-cathode cathode-neutralizer used had a length of 72 mm and operated with an electron emission of 10 A [10]. The magnets were selected to have a maximum variation in strength of less than ±3%.

The ion beam was characterized with a screened probe [11]. The screen in front of the collector was operated at a negative potential to reflect electrons. The collector was operated at ground potential for beam profile measurements and varied over a range of positive potentials for an energy analysis of the ions. To obtain a profile, the probe was moved through an arc of 180° with the center of the arc centered on the exit plane of the ion source and the probe collector 30 cm from the source. The probe was oriented toward the ion source, so that there was no significant departure from normal ion incidence.

A typical discharge voltage for an end-Hall ion source is 150 V, which results in a mean ion energy of 90-100 eV. The discharge current was therefore 2 A at the operating discharge power of 300 W. Beam profiles obtained at these discharge conditions are shown in Fig. 8 for a 30 cm probe distance. The maximum ion current at 0 degrees varied less than ±8% from the mean value. The ion-beam currents, integrated from these profiles, had a mean value of 0.47 A, with a variation of less than ±7%. The shape of these profiles corresponded to a beam-shape parameter, n, equal to 1.43.

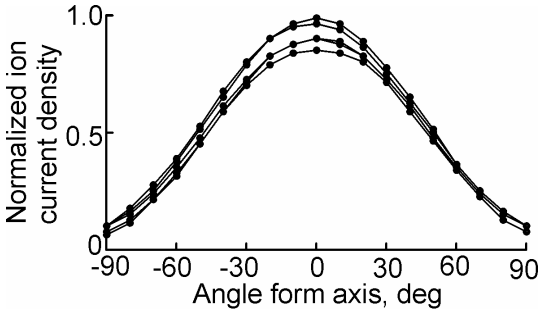

Figure 8. Normalized ion-beam profiles for the individual modules with a discharge of 150 V and 2 A .

FIVE-MODULE ARRAY PERFORMANCE

Five ion-source modules were assembled into a linear array. Passive flow restrictions were used to distribute approximately equal gas flows to the five ion-source modules. These restrictions consisted of sections of stainless steel tubing with an 1.6-mm outside diameter, approximately 30 cm long. The flow restrictions were inside the vacuum chamber so that only one gas feedthrough was required.

Theoretical calculations of the composite ion beam were carried out, using Eq. (2) to model the ion beam. A beam-shape parameter of 1.43, a target distance (S in Fig. 2) of 12 cm, and a 10-cm center-to-center module spacing were also used. These calculations showed that an increased length of ±5% uniformity was obtained by reducing the spacing for the end modules from 10 cm to 8 cm. (See the discussion of Fig. 7 for additional information on this effect.) Using the 8-cm spacing for the end modules, a theoretical distribution of ion current density was obtained and is indicated by the contour lines in Fig. 9.

Measuring the experimental distribution of ion current density required the use of a different probe. Screened probes have a vignetting correction for an off-normal angle of ion incidence on the probe. This correction was negligible for the probe surveys presented in Fig. 8, because the probes were always oriented toward the ion source. The ion current at almost any location on the workpiece,

47th Annual Technical Conference Proceedings (2004) ISSN 0737-5921

however, would include significant contributions from at least two modules at different locations, so that an explicit single-valued vignetting correction was not possible.

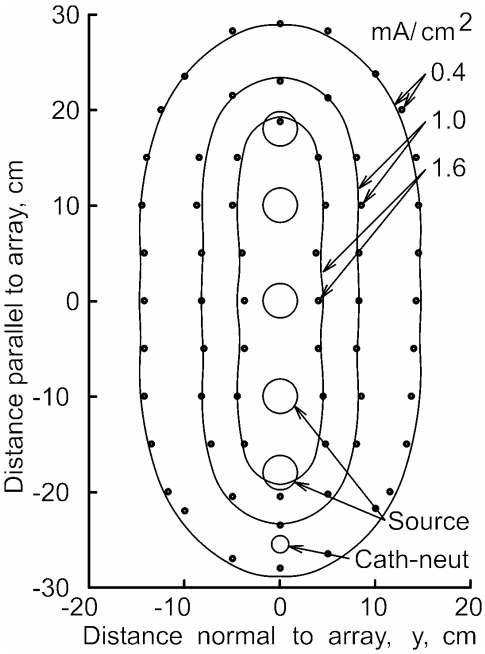

Figure 9. Distribution of ion current density at a distance of 12 cm from the five-module linear array. Contours are theoretical, solid circles are experimental.

To overcome the problem of the vignetting correction, planar probes [11] were used in measuring the ion current density from the linear modular ion-source array. With the collectors oriented parallel to the simulated workpiece surface, the geometric correction for off-normal incidence is incorporated automatically. However, a planar probe has an additional error due to secondary electron emission from the collisions of ions with the collector surface. At the negative potential necessary to prevent ion-beam electrons from reaching the collectors, the secondary electrons escape from the collector and result in a current that is indistinguishable from that of arriving ions. In addition, when measuring the current of low-energy ions, the trajectories of these ions are deflected by the probe potential to artificially increase the number of ions collected. This effect can be reduced by using a guard ring around the collector at the same potential as the collector. All errors included, the indicated ion current density from a low-energy ion beam can approach twice the true value. To correct for these errors, the current densities from the planar-probe surveys of the ion-beam profiles were reduced by the ratio of screened to planar probe readings obtained with a single ion-source module at the same operating conditions and normal ion incidence.

Using this correction, the experimental current densities were measured at a distance of 12 cm on 5-cm centers both parallel and normal to the length of the ion-source array. The locations at current densities of 8, 20, and 32 mA/cm^2 were obtained by interpolating between the measurements taken on 5-cm centers. These locations are shown as solid circles in Fig. 9 and are in excellent agreement with the theoretical contours. The discharge was 150 V, 10 A (total).

Figure 9 shows the ion-beam distribution at the workpiece, but it cannot directly be used to calculate dose or show uniformity. For these purposes, the integral form shown in Figs. 5-7 is more useful. At each location along the beam length, the current density is integrated with Eq. (1). The integral values are shown in Fig. 10, for both the theoretical calculation (continuous line) and the numerically integrated experimental values (circles). The length of ±5% uniformity is about 30 cm, which compares favorably with the overall center-to-center length of the array of 36 cm.

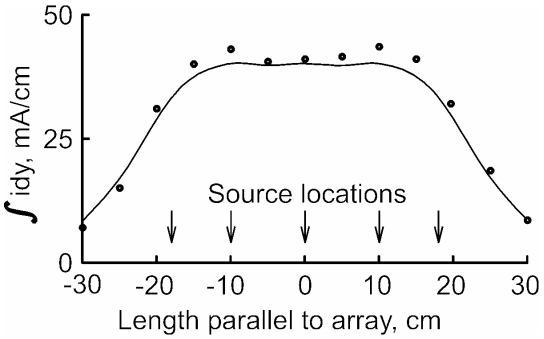

Figure 10. Distribution of current-density integral over the length of the ion source at a distance of 12 cm from the five-module linear array. Contour is theoretical, solid circles are experimental.

A cleaning example can be given for the use of Fig. 10. The value of the integral in Fig. 10 is about 40 mA/cm in the uniform central region. A nominal cleaning dose is a number of ions equal to the atomic sites on the surface being cleaned. This is approximately 0.16 mA-s/cm^2 [12]. From Eq. (1), this dose can be satisfied with an integral of 40 mA/cm using a workpiece velocity of 250 cm/sec or less. This is a nominal dose. A specific cleaning application may require a larger or smaller dose, hence permit a smaller or larger workpiece velocity.

47th Annual Technical Conference Proceedings (2004) ISSN 0737-5921

The difference between the theoretical and experimental values is not large, but is easily explained by the somewhat approximate nature of beam-shape model used (Eq. (2)) and the selection procedure for the beam-shape parameter. What is more significant is the agreement between theoretical and experimental values. This agreement validates the modeling approach used, which assumes that the overall composite ion beam can be calculated by superposition of the ion beams from the individual modules. In addition, the overlapping ion beams of the individual modules gives a greater uniformity of the linear array than was obtained in the tests of the individual modules.

Operational limits were also investigated. With the emission of the cathode-neutralizer established before the discharge was started, the discharge was initiated at all modules as long as the discharge voltage was 80 V or more. After starting the discharge, operation was stable for discharges from about 50 V to over 200 V. The distribution of discharge currents between the modules varied over the operating voltage range, but stayed within the initial range of ±8%.

CONCLUDING REMARKS

A design procedure is described for a modular linear ion source. Using this procedure, a five-module linear array was designed and tested. The overall center-to-center length of the array was 36 cm. The center 30 cm of this length provided a ±5% uniformity.

Operation of the five-module array with the cathode-neutralizer at one end assures operation of a ten-module array with a centrally mounted cathode-neutralizer. Using the same spacing for the central modules, the ten-module array would be expected to have an overall center-to-center length of 86 mm and a ±5% uniformity over the central 80 cm.The module power level (presently about 300 W) could easily be increased by using larger modules. The overall power level is presently limited by the maximum cathode-neutralizer emission of 10 A, but could easily be extended to 20 A by using a larger cathode-neutralizer [12]. In a similar manner, larger modules could be used where higher power levels are required.

In summary, the modular approach to a linear ion source permits rapid and economical design to a wide range of ion-source lengths and powers. These capabilities should extend the capabilities of existing linear ion sources.

REFERENCES

1. H.R. Kaufman, R.S. Robinson, and R.I. Seddon, "End-Hall Ion Source," *J. of Vacuum Science and Technology*, A5 (4), 2081, 1987

.

2. H.R. Kaufman and R.S. Robinson, U.S. Patent 4,862,032, "End-Hall Ion Source," Aug. 29, 1989.

3. H.R. Kaufman, U.S. Patent 6,608,431, "Modular Gridless Ion Source," Aug. 19, 2003.

4. H.R. Kaufman, "Technology of Electron-Bombardment Thrusters," *Advances in Electronics and Electron Physics*, Vol. 36 (L. Marton, ed.), p. 265, Academic Press, New York, 1974

5. V.V. Zhurin, H.R. Kaufman, and R.S. Robinson, "Physics of Closed Drift Thrusters," *Plasma Sources Science and Technology*, 8 (1), R1, 1999.

6. J.M.E. Harper, J.J. Cuomo, and H.R. Kaufman, "Technology and Applications of Broad-Beam Ion Sources," *J. of Vacuum Science and Technology*, 21 (3), 737, 1982

7. H.R. Kaufman and J.M.E. Harper, "Ion Doses for Low-Energy Ion-Assist Applications," *J. of Vacuum Science and Technology*, A22 (1), 221, 2004.

8. H.R. Kaufman and R.S. Robinson, *Operation of Broad-Beam Ion Sources*, p. 65, Commonwealth Scientific Corporation, Alexandria, Virginia, 1987.

9. Model EH200 end-Hall ion source, Kaufman & Robinson, Inc.

10. Model SHC1000 hollow-cathode electron source, *Ibid*.

11. Ref. 8, p.99.

12. Model MHC5000 hollow-cathode electron source, Kaufman & Robinson, Inc.

47th Annual Technical Conference Proceedings (2004) ISSN 0737-5921